

e/p Separation Study Using the ISS-CREAM Top and Bottom Counting Detectors

S. C. Kang*^{†1}, Y. Amare², D. Angelaszek^{2,3}, N. Anthony³, G.H. Choi⁴, M. Chung², M. Copley², L. Derome⁵, L. Eraud⁵, C. Falana², A. Gerrety², L. Hagenau³, J.H. Han², H.G. Huh², Y.S. Hwang¹, H.J. Hyun¹, H.B. Jeon¹, J.A. Jeon⁴, S. Jeong⁴, H.J. Kim¹, K.C. Kim², M.H. Kim², H.Y. Lee⁴, J. Lee^{1,4}, M.H. Lee², C. Lamb², J. Liang³, L. Lu³, J.P. Lundquist^{2,4}, L. Lutz², B. Mark², A. Mechaca-Rocha⁶, T. Mernik², M. Nester³, O. Ofoha², H. Park¹, I.H. Park⁴, J.M. Park¹, N. Picot-Clemente², S. Rostsky², E.S. Seo^{2,3}, J.R. Smith², R. Takeishi⁴, T. Tatoli², P. Walpole², R.P. Weinmann², J. Wu², Z. Yin^{2,3}, Y.S. Yoon^{2,3}, H.G. Zhang²

¹ Dept. of Physics, Kyungpook National University, Daegu, Republic of Korea

² Inst. for Phys. Sci. and Tech., University of Maryland, College Park, MD, USA

³ Dept. of Physics, University of Maryland, College Park, MD, USA

⁴ Dept. of Physics, Sungkyunkwan University, Suwon, Republic of Korea

⁵ Laboratoire de Physique Subatomique et de Cosmologie, Grenoble, France

⁶ Instituto de Fisica, Universidad Nacional Autonoma de Mexico, Mexico

Cosmic Ray Energetics And Mass for the International Space Station (ISS-CREAM) is an experiment for studying the origin, acceleration, and propagation mechanisms of high-energy cosmic rays. The ISS-CREAM instrument was launched on the 14th of August 2017 to the ISS aboard the SpaceX-12 Dragon spacecraft. The Top and Bottom Counting Detectors (TCD/BCD) are parts of the ISS-CREAM instrument and designed for studying electron and gamma-ray physics. The TCD/BCD each consist of an array of 20×20 photodiodes on a plastic scintillator. The TCD/BCD can separate electrons from protons by using the difference between the shapes of electromagnetic and hadronic showers in the high energy region. The Boosted Decision Tree (BDT) method, which is a deep learning method, is used in this separation study. We will present results of the electron/proton separation study and rejection power in various energy ranges.

*36th International Cosmic Ray Conference -ICRC2019-
July 24th - August 1st, 2019
Madison, WI, U.S.A.*

[†]sinchul1216@gmail.com

[‡]Speaker for the ISS-CREAM Collaboration[§]

[§]For the collaboration list see PoS(ICRC2019)1177

*Speaker.

1. Introduction

The ISS-CREAM detector was launched on the 14th of August 2017 (EDT) to the ISS aboard the SpaceX-12 Dragon spacecraft. The ISS-CREAM detector can measure cosmic-ray protons from 1 TeV to 1,000 TeV. By measuring these high energy cosmic-ray particles, the keys to answer unsolved questions, such as origin and propagation of cosmic ray particles may be found.

The ISS-CREAM detector is composed of a Silicon Charge Detector (SCD), a calorimeter (CAL), the Top and Bottom Counting Detectors (TCD/BCD) and a Boronated Scintillator Detector (BSD) as shown in Fig. 1. The SCD measures charges and the CAL measures the energies of the cosmic-ray. The TCD/BCD can separate electrons from hadrons using their different shower shapes, and the BSD can also separate hadrons using thermal neutron produced in the CAL.

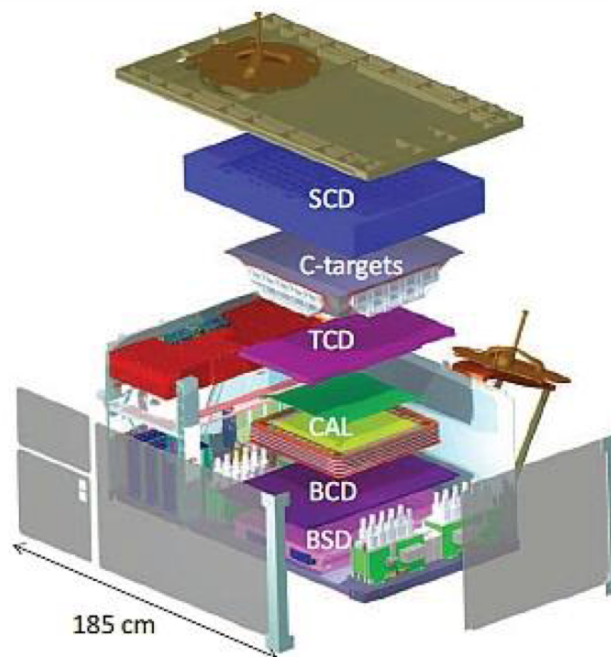


Figure 1: Schematic of the ISS-CREAM instrument, composed of the SCD, carbon targets, TCD/BCD, CAL, and BSD [1]

2. Top and Bottom Counting Detectors

The TCD is placed above the CAL and the BCD is below the CAL. The size of the TCD is $901 \times 551 \text{ mm}^2$ and the BCD is $950 \times 650 \text{ mm}^2$. The height of the TCD is 30 mm and the BCD is 33 mm. The TCD/BCD are composed of 20×20 photodiodes arrays and plastic scintillators. The active area of the photodiodes is $20 \times 20 \text{ mm}^2$ with a thickness of $650 \mu\text{m}$. The dimensions of the plastic scintillators for the TCD/BCD are $500 \times 500 \times 5 \text{ mm}^3$ and $600 \times 600 \times 10 \text{ mm}^3$, respectively.

Due to the active area of the photodiodes arrays and their location, the TCD/BCD can measure the longitudinal and lateral profiles of the showers. Electromagnetic showers are narrower and

more easily depleted than hadronic showers. Thus, TCD/BCD can separate electrons from hadrons using their different shower shapes.

The TCD/BCD can also provide a low energy trigger. There are fourteen VA/TA chips in each TCD/BCD as shown in Fig. 2. Only two VA/TA chips in middle of the two mother boards are connected to twenty photodiodes, while other VA/TA chips are connected to thirty photodiodes. The TCD/BCD trigger is designed to respond to events with a signal above threshold in at least one VA/TA chip in the TCD and at least two VA/TA chips in the BCD.

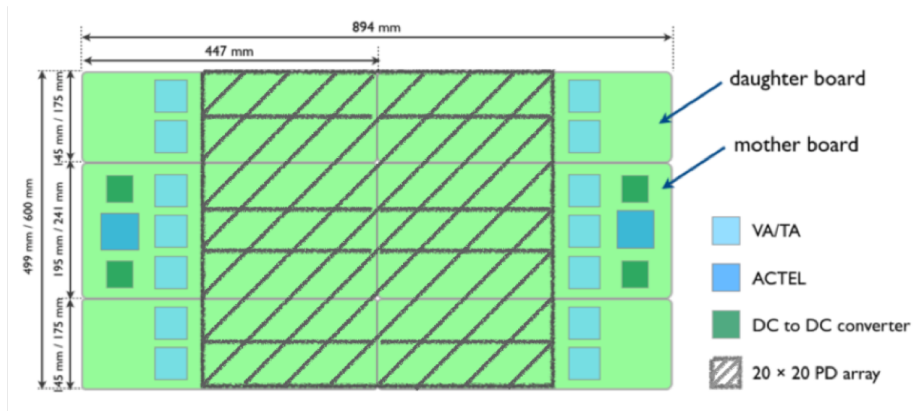


Figure 2: A schematic of the TCD/BCD with a layout of its electronics components. Twenty photodiodes are connected to the middle of VA/TA chip in the mother board, thirty photodiodes are connected to each other VA/TA chips [2]

2.1 Performance of the TCD/BCD on the ISS

During the flight, we monitored the pedestal RMS and charge gain values of the TCD/BCD. As shown in Fig. 3, the pedestal RMS of the TCD/BCD was stable during the flight and smaller than 20 ADC. Also, we checked the RMS values of each channel when the ISS passes through the South Atlantic Anomaly (SAA). In the SAA, the detectors are exposed to proton rates of $\sim 4000/(\text{s} \times \text{cm}^2 \times \text{sr})$ with ~ 20 MeV [3]. When the ISS passes through the SAA, ISS-CREAM had initially turned off to avoid the radiation damage. However, the ISS-CREAM was turned on to check the status of each detector in November 2017. The pedestal RMS distribution of TCD/BCD didn't change before or after SAA transits as shown in Fig. 4.

Each TCD/BCD channel is calibrated using a known amount of charge. The gain of the channel is defined as the ratio of the response value (ADC) to the input charge (DAC). The most channels in the TCD/BCD show similar charge gain values with an average of 324 ADC/DAC for both as shown in Fig. 5.

The TCD/BCD can measure the position of the cosmic-ray particles using their 20×20 photodiodes arrays. Since CAL is located between the TCD and the BCD, the track information of cosmic ray particles in the CAL is a good reference to confirm the hit positions in the TCD/BCD. The position of TCD/BCD is calculated using energy weighted average position. Fig. 6 shows scatter plots of the TCD/BCD hit positions using extrapolated tracks in the CAL and energy weighted average position with good linear correlation. The 1σ value of the differences in the two positions

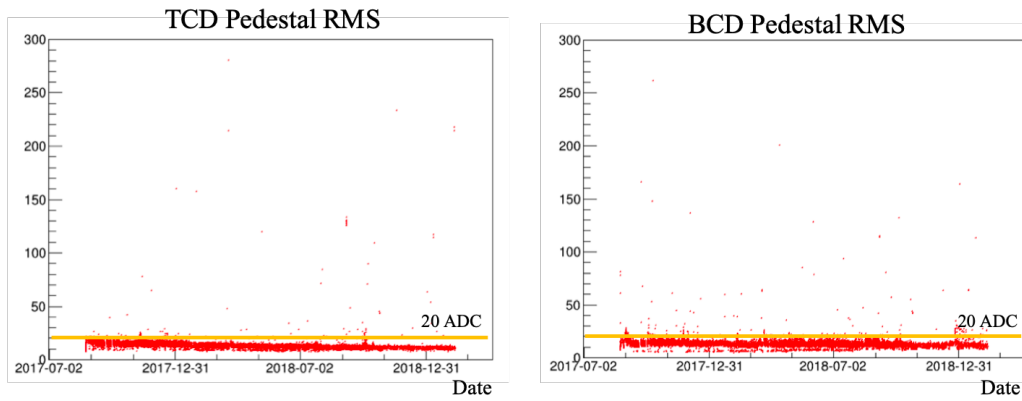


Figure 3: Pedestal RMS values of one channel in the TCD/BCD. The pedestal RMS values are stable from deployment up to shutdown in February 2019 and less than 20 ADC.

in the TCD is 67.9 mm along the x axis and 64.9 mm along the y axis. In the BCD, the 1σ position difference is 63.0 mm along the x and y axes.

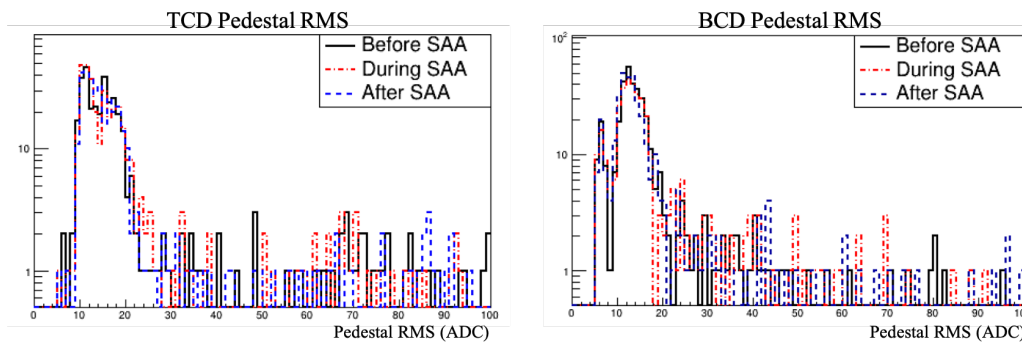


Figure 4: The TCD pedestal RMS distribution before, during and after SAA (left), and those of BCD (right). The pedestal distribution of the detectors are almost same before and after each SAA period.

3. *e/p* Separation

Because the protons are the dominant component in cosmic ray particles [4], one of the most important things in studying electron spectrum is separation of electrons from the protons. The electrons and proton can't be separated using the SCD, since they have the same absolute charge. The TCD/BCD can separate electrons from protons using the difference between electromagnetic showers and hadronic showers.

3.1 Event Selection

Before separating electrons from protons, we need to select meaningful data. To select charge 1 particles, the data which have SCD charge values from 0.3 to 1.7 are selected. To exclude noise events, the events which didn't pass the trigger condition are removed, and events triggered within the SAA region are also removed. Also, the time periods that have higher trigger rates than normal

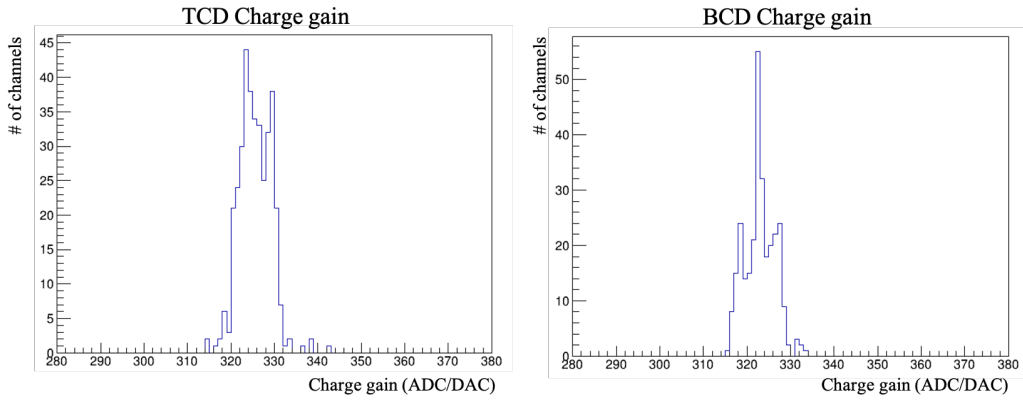


Figure 5: Each channel of TCD/BCD has similar charge gain value. The mean of charge gain values of TCD/BCD is 324 ADC/DAC.

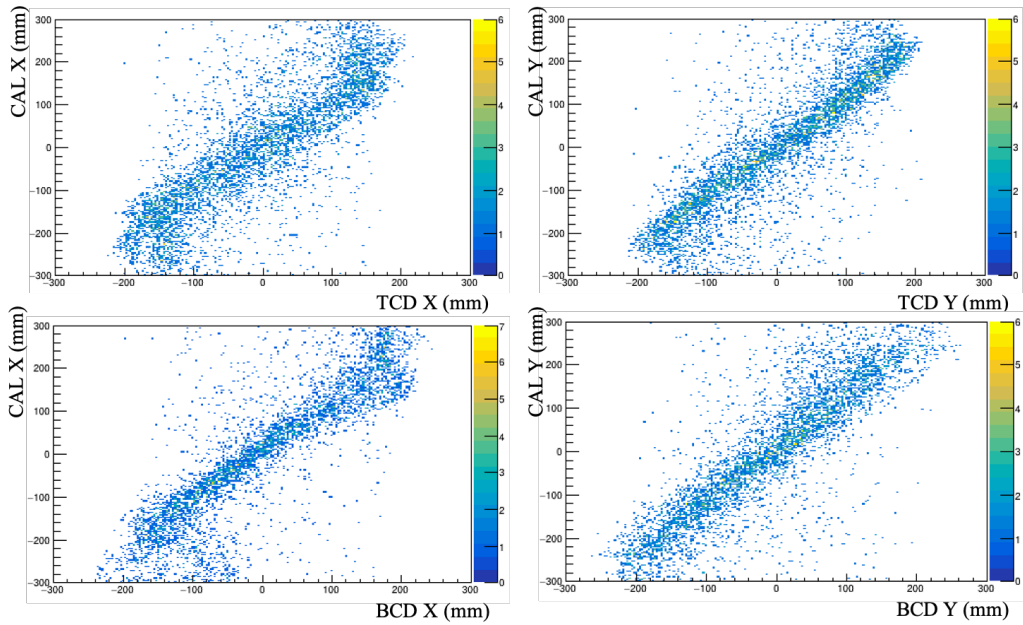


Figure 6: Scatter plots of TCD/BCD hit positions. The CAL X, Y are hit positions in the TCD/BCD using extrapolated tracks in the CAL. The TCD/BCD X, Y are energy weighted average position in TCD/BCD. These two estimated hit positions show a strong linear correlation.

condition are excluded. Therefore, the events which were triggered when the TCD/BCD bias voltages are off or pedestal data are abnormal are removed.

3.2 Boosted Decision Tree

The Boosted Decision Tree (BDT) is a machine learning method [5]. A decision tree is a sequence of binary splits of the data. Repeated decisions are made on a single variable at a time until a stop criterion is fulfilled. A single decision tree is unstable since the small fluctuations in training data can make large differences in results. Boosting is used to improve the instability of

a single decision tree. For boosting, the training data which are misclassified have their weights increased, and a new tree is formed. This procedure is then repeated for the new tree.

In this study, the shower distribution, the number of hits, and deposited energy in the TCD/BCD are used. The proton and electron data simulated by the Geant3 Monte-Carlo (MC) are used for BDT training. The energy of the proton data starts from 300 GeV and follows a power law distribution with a -2.7 spectrum index. The energy of the electron data starts from 100 GeV and follows a power law distribution with a -3.0 spectrum index. The Fig. 7 shows BDT test results distribution with deposited energy in CAL.

The BDT was trained in three energy regions from 150 GeV to 300 GeV. The Fig. 8 shows the BDT variable distribution from 189 GeV to 238 GeV. The trained MC BDT is well matched with the ISS data BDT distribution and electrons are well separated from protons. In the BDT distribution, approximately $\sim 75\%$ events are protons and $\sim 25\%$ are electrons.

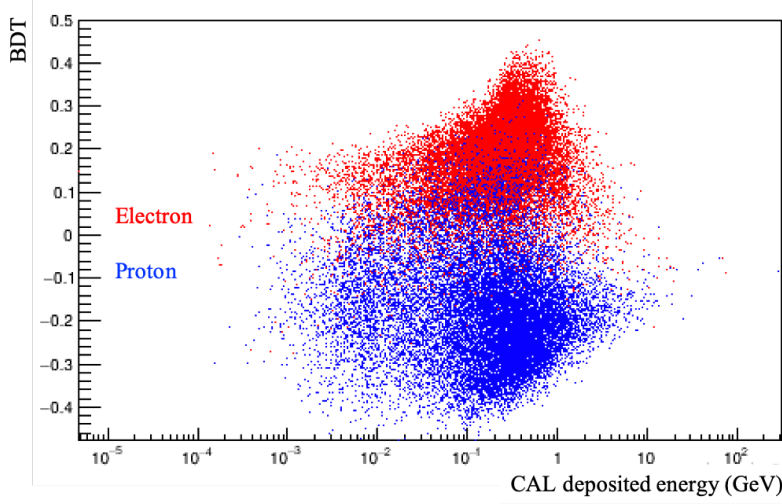


Figure 7: The distribution of the MC BDT test result with respect to CAL deposited energy. The red dots are electrons and blue dots are protons. Electrons have a BDT variable value close to 1 and proton have a BDT value close to -1.

4. Results

The rejection power (RP) was calculated using fractions of electrons and protons to total number of events as defined in [6]. We choose the BDT cut value when the number of electrons is 90% in each energy region. The CALET electron spectrum [7] is used to get $N_{e\ total}$ in each energy region and the AMS-02 proton spectrum data [8] is used to get $N_{p\ total}$ in the energy region from 150 GeV to 900 GeV. We study the rejection power in several electron energy regions (150 GeV – 189 GeV, 189 GeV – 238 GeV, 238 GeV – 300 GeV). The electrons and protons that have a BDT variable value larger than the BDT cut value are selected in each energy region. The proton rejection power from 150 GeV to 189 GeV of electrons is $(1.0 \pm 0.4) \times 10^4$, from 189 GeV to 238 GeV it is $(2.2 \pm 0.9) \times 10^4$, and from 238 GeV to 300 GeV it is $(6.4 \pm 1.7) \times 10^3$. These proton rejection power results show similar values to the previous MC studies [9].

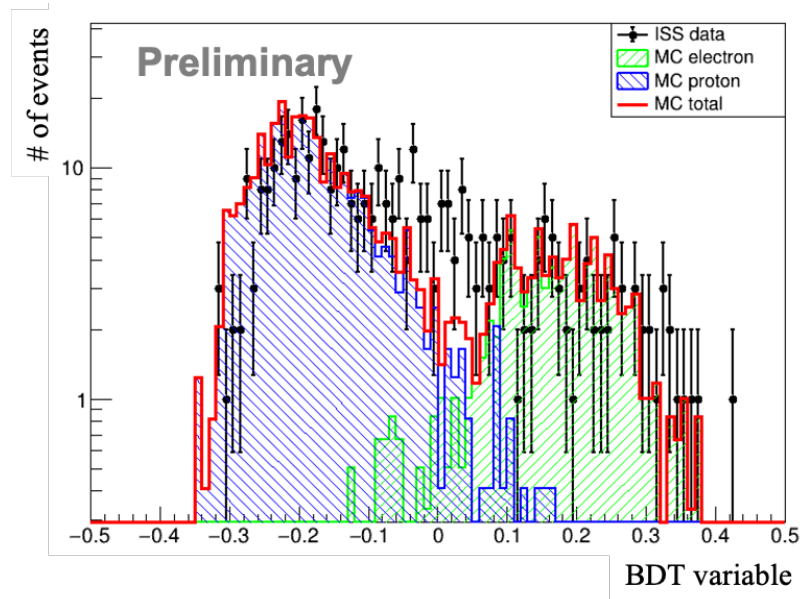


Figure 8: The BDT variable distribution from 189 GeV to 238 GeV electrons for ISS data and MC. The black dots are data taken on the ISS. Blue and green histograms are proton and electron MC. The red histogram is total MC. Data appears to consist of approximately $\sim 75\%$ protons and $\sim 25\%$ electrons.

5. Conclusion

The TCD/BCD, one of the detectors in ISS-CREAM instrument, is working well on the ISS. The pedestal RMS and charge gain values are stable. The hit positions in the TCD/BCD and CAL reconstructed cosmic ray particles' tracks show good correlation. Also, the TCD/BCD status were normal during the SAA periods.

One of the goals of the TCD/BCD is separating electrons from protons. In this study, we get the proton rejection power in three energy regions, 150 GeV – 189 GeV, 189 GeV – 238 GeV and 238 GeV – 300 GeV. The RP in each energy region is 1.0×10^4 , 2.2×10^4 and 6.4×10^3 . This preliminary result is comparable to previous MC studies. In this study, the improved CAL track reconstruction method, CAL energy calibration, TCD/BCD energy calibration, and SCD charge reconstruction aren't applied yet. We will study e/p separation in higher energy region, and add BDT training variable using CAL data.

Acknowledgments

This work was supported in the U.S. by NASA grant NNX17AB41G, in Korea by MSIT under the High-Potential Individuals Global Training Program (2019-0-01578) supervised by the IITP, and by National Research Foundation grants 2018R1A2A1A05022685 and 2018R1A6A1A06024970, and their predecessor grants. It was also supported in France by IN2P3/CNRS and CNES and in Mexico by DGAPA-UNAM project IN109617. The authors thank NASA GSFC WFF and its contractors for engineering support and project management, JSC ISS Program Office for the

launch support and ISS accommodation, MSFC for the operational support, and KSC and SpaceX for the launch support.

References

- [1] E. S. Seo et al., *Adv. Space Res.* **53**, No. 10, 1451 (2014).
- [2] H. J. Hyun et al., *Nucl. Instrum. Methods Phys. Res. A*, **787**, 134 (2015)
- [3] G. P. Ginet et al., *IEEE Radiation Effects Data Workshop*, **0**, 1 (2007)
- [4] R. A. Mewaldt, *Adv. Space Res.* **14**, No. 10, 737 (1994).
- [5] P. Speckmayer et al., *J. Phys.Conf. Ser.* **219**, 032057 (2010)
- [6] F. Palma et al., *In Proceeding of the 34th International Cosmic Ray Conference* **236** 1196 (2015)
- [7] O.Andrani et al., *Phys. Rev. Lett.* **120**, 261102 (2018)
- [8] M. Aguilar et al., *Phys. Rev. Lett.* **114**, 71103 (2015)
- [9] J. M. Park et al., *Adv. Space Res.* **62**, 2939 (2017)